4. CONCLUSION

A novel compact microstrip bandpass filter with two or three transmission zeros has been developed by combining parallel coupling and end coupling. By giving two or three transmission paths to the signals, two or three transmission zeros have been realized. Experimental bandpass filters have been fabricated and measured, and the simulation and measurement results show the electrical performances to be almost in agreement.

REFERENCES

1. J.-R. Lee, J.-H. Cho, and S.-W. Yun, New compact bandpass filter using microstrip λ/4 resonators with open stub inverter, IEEE Microwave Guided Wave Lett 10 (2000), 526–527.
2. L. Zhu and W. Menzel, Compact microstrip bandpass filter with two transmission zeros using a stub-tapped half-wavelength line resonator, IEEE Microwave Wireless Compon Lett 13 (2003), 16–18.
3. J.S. Hong and M.J. Lancaster, End-coupled microstrip slow-wave resonator filter, Electron Lett 32 (1996), 1494–1496.

A FULLY INTEGRATED 5.2-GHz SINGLE-ENDED-IN AND SINGLE-ENDED-OUT 0.18-μm CMOS GILBERT UPCONVERTER

C. C. Meng,[1] M. Q. Lin,[1] and G. W. Huang[2]
[1] Department of Communication Engineering
National Chiao Tung University
Hsinchu, Taiwan, Republic of China
[2] National Nano Device Laboratories
Hsinchu, Taiwan, Republic of China

Received 3 April 2004

ABSTRACT: *A monolithic 5.2-GHz single-ended-in and single-ended-out Gilbert upconverter with balanced operation is demonstrated using 0.18-μm deep n-well CMOS technology. The fully matched Gilbert upconverter has conversion gain of −11.5 dB and OP_{1dB} of −19 dBm when input IF = 300 MHz, LO = 4.9 GHz, and output RF = 5.2 GHz. The IF input return loss is better than 14 dB for frequencies up to 7 GHz, while RF output return loss is 15 dB at 5.2 GHz.* © 2004 Wiley Periodicals, Inc. Microwave Opt Technol Lett 43: 240–242, 2004; Published online in Wiley InterScience (www.interscience.wiley.com). DOI 10.1002/mop.20430

Key words: *CMOS; Gilbert upconverter; RFIC*

INTRODUCTION

A fully matched Gilbert upconversion micromixer output is demonstrated at 5.2 GHz using 0.18-μm deep n-well CMOS technology. The circuit schematic is shown in Figure 1. A Gilbert micromixer [1] intrinsically has a single-ended input. The single-to-differential input stage of a Gilbert micromixer not only transforms an unbalanced signal into balanced signals, but also provides wideband impedance matching. A passive LC current combiner is applied at the upconversion-mixer output stage. An LC combiner has the ability to double the output current and converts the differential outputs into a single-ended output [2]. As illustrated in Figure 1, the upconversion micromixer consists of an LO Gilbert mixer core, a single-to-differential IF input, and an RF-output LC-current combiner with lowpass LC matching. The LO input signal is generated by a broadband 180° coupler in order to maintain balanced LO signals. Thus, the truly balanced operation of a CMOS Gilbert micromixer with a single-ended input and a single-ended output is achieved in this paper.

A double-balanced Gilbert mixer has been widely used in RF IC design due to the excellent port-to-port isolation property. The separate feeding ports for IF (RF) and LO in a Gilbert upconverter (downconverter) provides good isolation between IF (RF) port and LO port. If the IF (RF) and LO signals that feed the Gilbert mixer are balanced, the IF-RF (RF-IF) and LO-RF (LO-IF) port-to-port isolation will be excellent in a Gilbert upconverter (downconverter). Of course, this fact will be observed when the output signals are taken differentially [3, 4]. When the input signals are no longer balanced, good isolation properties can be accomplished if the Gilbert cell circuitry possesses good common-mode rejection. However, the common-mode rejection provided by the biased current source in a conventional Gilbert mixer deteriorates rapidly at high frequencies.

CIRCUIT DESIGN

A photograph of the fabricated circuit is shown in Figure 2. The die size is 0.93 × 0.96 mm^2. In order to implement the circuit, 0.18-μm deep n-well CMOS technology is used. The common-gate-biased transistor M_3 and common-source-biased transistor M_2 provide 180° out-of-phase transconductance gain when M_1 and M_2 are connected as a current mirror. All the NMOS transistors are in the deep n-wells to improve isolation; also, M_3 does not have the physical capability to cause an unbalance in the transconductance gain [5]. The common-gate-configured transistor M_3 possesses good frequency response, while the speed of common-source-configured M_2 is improved drastically by adding a low-impedance diode-connected M_1 at the input of the common-source-configured M_2.

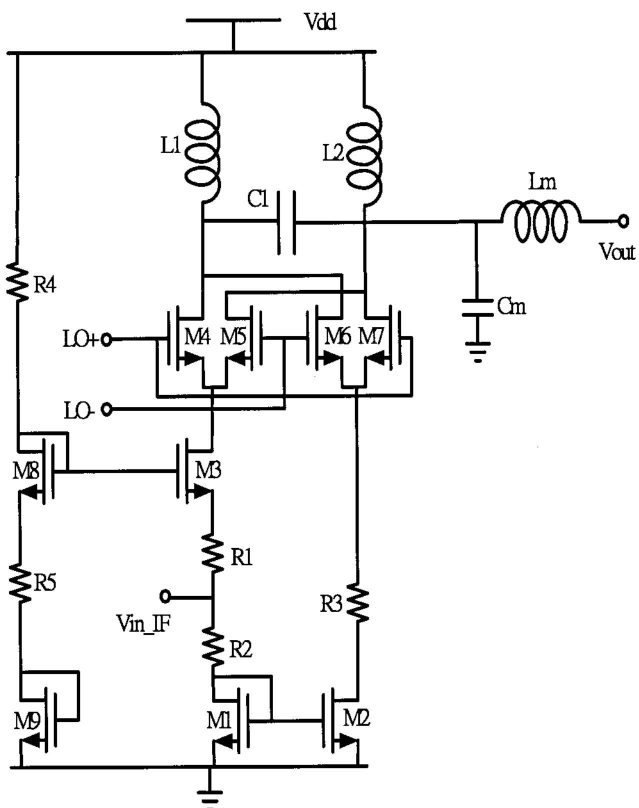

Figure 1 Schematic diagram of the single-ended-in and single-ended-out CMOS Gilbert upconverter under truly balanced operation

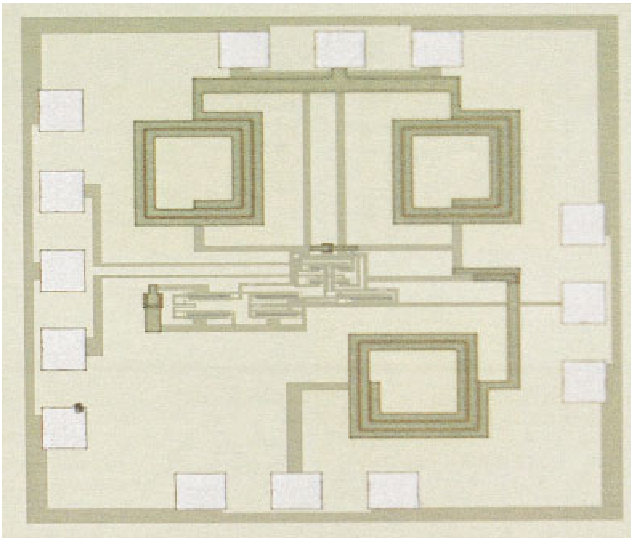

Figure 2 Photograph of the single-ended-in and single-ended-out CMOS Gilbert upconverter. [Color figure can be viewed in the online issue, which is available at www.interscience.wiley.com.]

The CMOS Gilbert mixer core consists of transistors M_4, M_5, M_6, and M_7. The current combiner doubles the output current at the following resonant frequency:

$$\omega_0 = \sqrt{\frac{1}{2L_1C_1}}.$$

Thus, an integrated passive LC current combiner at 5.2 GHz is designed in this paper. There are three rectangular on-chip inductors (all at 2.36 nH with 2.5 turns) in the die photograph of Figure 2. A lowpass LC network consisting of inductor L_m and capacitor C_m is used to improve the output matching, as illustrated in Figure 1. The LC current combiner and the LC low-pass network are designed to form a band-pass matching network and the designed center frequency is located at 5.2 GHz.

EXPERIMENTAL RESULTS

The CMOS Gilbert upconverter with a single-ended input and a single-ended output also facilitates on-wafer RF measurement. The input GSG IF port is on the right side of the die, while the output GSG RF port is on the bottom. The LO GSGSG signal port is on the left side of the die and the DC pads are on the top. The supply voltage is 1.8 V and the current consumption is 2.6 mA. The measured conversion gain as a function of LO power is shown in Figure 3. As shown in the figure, the peak conversion gain is −11.5 dB when LO power is around 0 dBm and LO = 4.9 GHz. Figure 4 shows the IF input return loss and the RF output return loss. The output RF return loss is 15 dB at 5.2 GHz and the IF input return loss is better than 14 dB or frequencies up to 7 GHz. The power performance of the upconverter is shown in Figure 5. The experiment shows that the OP_{1dB} is −19 dBm. The measured data show that LO-RF isolation is better than 28 dB at LO frequencies from 4.0 to 6.0 GHz. The high-isolation property may be due to the truly balanced operation of the Gilbert micromixer with the output LC current combiner. The LO-IF isolation is better than 30 dB at LO frequencies from 4.0 to 6.0 GHz.

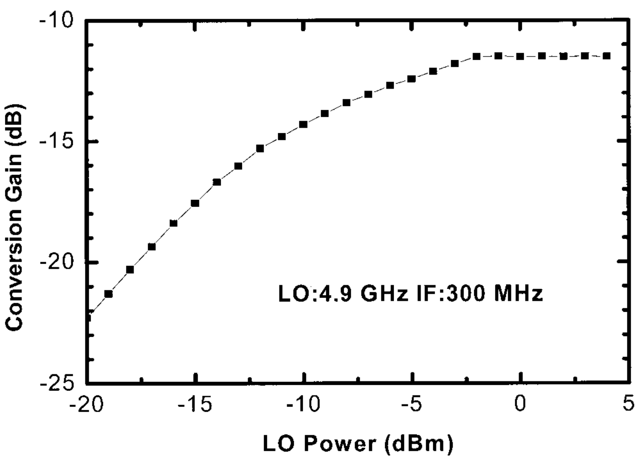

Figure 3 Conversion gain vs. LO power measurement of the single-ended-in and single-ended-out CMOS Gilbert upconverter

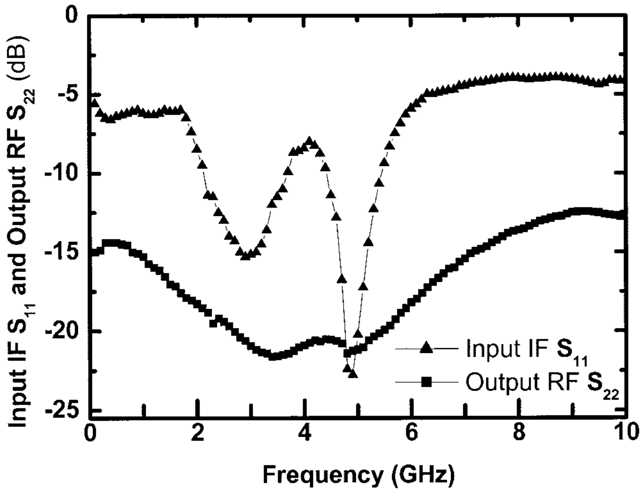

Figure 4 IF-port input return loss and RF-port output return loss of the single-ended-in and single-ended-out CMOS Gilbert upconverter

CONCLUSION

A truly balanced operation of a Gilbert micromixer with single-ended input and output has been demonstrated using 0.18-μm deep

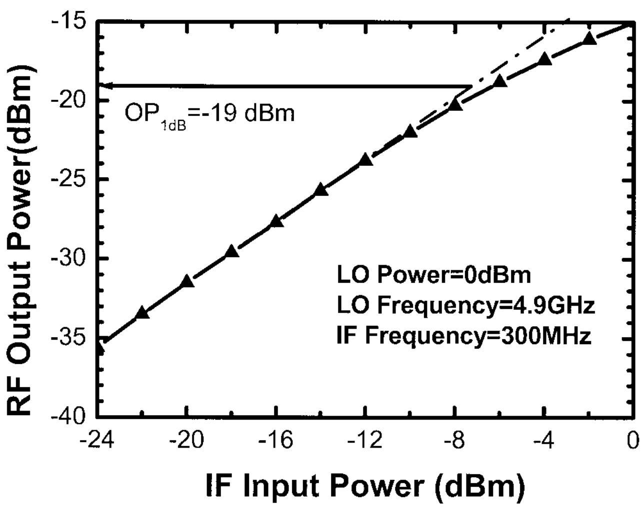

Figure 5 Power performance of the single-ended-in and single-ended-out CMOS Gilbert upconverter

n-well CMOS technology. The fully integrated CMOS upconverter has conversion gain of −11.5 dB and OP_{1dB} of −19 dBm when input IF = 0.3 GHz, LO = 4.9 GHz, and RF = 5.2 GHz. The IF input return loss is better than 14 dB for frequencies up to 7 GHz while RF output return loss is 15 dB at 5.2-GHz output frequency.

ACKNOWLEDGMENTS

Support from the National Science Council (contract no. NSC 92-2219-E-009-023), Ministry of Education (contract no. 89-E-FA06-2-4), and Ministry of Economics Affairs (contract no. 92-EC-17-A-05-S1-020) is highly appreciated.

REFERENCES

1. B. Gilbert, The Micromixer: A highly linear variant of the Gilbert mixer using a bisymmetric Class-AB input stage, IEEE J Solid-State Circ 32 (1997), 1412–1423.
2. J. Durec, An integrated silicon bipolar receiver subsystem for 900 MHz ISM band applications, IEEE J Solid-State Circ 33 (1998), 1352–1372.
3. C.C. Meng, S.S. Lu, M.H. Chiang, and H.C. Chen, DC to 8 GHz 11-dB gain Gilbert micromixer using GaInP/GaAs HBT technology, Electron Lett 39 (2003), 637–638.
4. C.C. Meng, S.K. Hsu, A.S. Peng, S.Y. Wen, and G.W. Huang, A fully integrated 5.2 GHz GaInP/GaAs HBT upconversion micromixer with output LC current combiner and oscillator, IEEE MTT-S Int Microwave Symp, 2003, Philadelphia, PA pp. A205–A208.
5. C.C. Meng, S.K. Xu, T.H. Wu, M.H. Chao, and G.W. Huang, A high-isolation CMFB downconversion micromixer using 0.18-μm deep n-well CMOS technology, IEEE MTT-S Int Microwave Symp, 2003, Philadelphia, PA pp. A105–A108.

CHARACTERIZATION OF PERIODIC MICROSTRIP-LINE EBG STRUCTURES WITH IMPROVED BANDSTOP BEHAVIORS

Hang Wang and Lei Zhu
School of Electronic and Electrical Engineering
Nanyang Technological University
Singapore 639798

Received 18 April 2004

ABSTRACT: *Periodic microstrip-line electromagnetic band-gap (EBG) structures with improved bandstop behaviors are constituted by adding the backside aperture and widening the strip conductor regarding to the low- and high-impedance microstrip-line sections, respectively. Its characteristics are studied by using the finite-difference time-domain (FDTD) method. After our FDTD-derived results are independently verified by those from ADS for an initial EBG structure, extensive work is done to investigate the concerned bandstop behaviors versus strip/aperture widths and lengths in order to achieve a broadened and deepened frequency stopband.* © 2004 Wiley Periodicals, Inc. Microwave Opt Technol Lett 43: 242–244, 2004; Published online in Wiley InterScience (www.interscience.wiley.com). DOI 10.1002/mop.20431

Key words: *periodic microstrip line; electromagnetic band-gap (EBG); FDTD; backside aperture; stopband*

1. INTRODUCTION

Periodic transmission-line structures with inductive and/or capacitive loading in intervals were studied several decades ago and their fundamentals for planar filter design were summarized in the literature, for example, in [1]. In recent years, as photonic band-gap (PBG) material was invented in the optical field, much effort has been made in the microwave field to develop a variety of planar electromagnetic band-gap (EBG) structures [2, 3] that are intuitively viewed as periodic transmission lines [4, 5] with inductive loading in series. By etching out a certain portion of metallic ground underneath the strip conductor in periodical intervals, the so-called microstrip-line EBG structure with circular and rectangular aperture configurations were constructed in [2] and [3], respectively. Their electrical performances have been theoretically and experimentally characterized in terms of the S-parameters of an EBG device [2, 3] and unit-length transmission parameters of an EBG media [5].

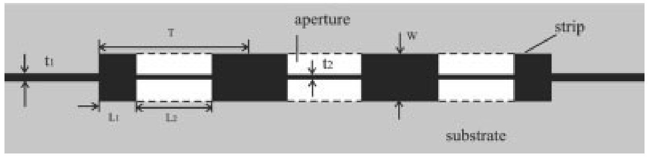

Figure 1 Geometry of the proposed periodic microstrip line EBG structure with finite cells of $N = 3$ and fixed sizes of $T = 5.6$ mm, $t_1 = 0.6$ mm, and $t_2 = 0.2$ mm

Based upon our previous work in the design of lowpass filters [6], an improved microstrip-line EBG structure is constructed by widening the strip width of a low-impedance section and formulating the backside aperture underneath the narrow strip of a high-impedance section, as illustrated in Figure 1. In order to characterize it in theory, a numerical finite-difference time-domain (FDTD) method [7] is developed with the use of Mur's absorbing boundary conditions (ABCs). After the accuracy of our FDTD code, as compared with the ADS simulation, is validated, the EBG structure is analyzed with respect to varied strip/aperture widths and length. Our optimized results demonstrate that the proposed EBG structure is able to significantly widen and deepen the stopband of our concern.

2. FDTD FORMULATION

The FDTD method proposed by Yee [7] has successfully gained a wide application in the modeling of various electromagnetic structures, including planar circuits and antennas. Its initial idea stemmed from the spatial and temporal derivative format of the well-known Maxwell's equations:

$$\nabla \times \vec{E} = -\mu \frac{\partial \vec{H}}{\partial t},$$

$$\nabla \times \vec{H} = \varepsilon \frac{\partial \vec{E}}{\partial t}. \tag{1}$$

As the exciting source is introduced, the electric and magnetic fields can be numerically derived as the direct solutions of these two coupled curl equations in both the space and time domains. The Yee's algorithm innovatively centers the relevant $\vec{E}$ and $\vec{H}$ vectors in the 3D space in such a way that every $\vec{E}$ vector is surrounded by its related four circulated $\vec{H}$ vector and vice versa. As such, it results in forming the so-called Yee's unit cell and updating the equations of the electric and magnetic fields in the time domain. Due to the length limitation, the two of six updating equations are only given below on the basis of the central-finite difference approach. Here, i, j, and k stand for the field-node